

Intramyocardial injection of hypoxia-conditioned extracellular vesicles increases myocardial perfusion in a swine model of chronic coronary disease



Dwight D. Harris, MD, Sharif A. Sabe, MD, Mark Broadwin, MD, Christopher Stone, MD, Cynthia Xu, MD, Meghamsh Kanuparth, MD, Akshay Malhotra, M. Ruhul Abid, MD, PhD, and Frank W. Sellke, MD, FACS

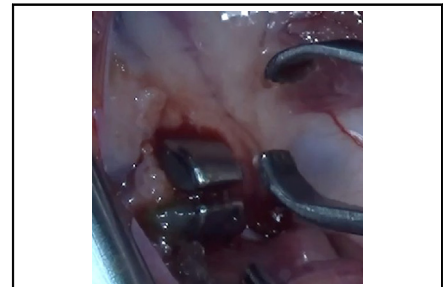
ABSTRACT

Objective: Coronary artery disease remains a leading cause of morbidity and mortality worldwide. Patients with advanced coronary artery disease who are not eligible for endovascular or surgical revascularization have limited options. Extracellular vesicles have shown potential to improve myocardial function in preclinical models. Extracellular vesicles can be conditioned to modify their components. Hypoxia-conditioned extracellular vesicles have demonstrated the ability to reduce infarct size and apoptosis in small animals. Our objective is to assess the potential benefits of hypoxia-conditioned extracellular vesicles in a large animal model of coronary artery disease.

Methods: Coronary artery disease was induced in 14 Yorkshire swine by ameroid constriction of the left circumflex coronary artery. Two weeks postsurgery, swine underwent a repeat left thoracotomy for injections of hypoxia-conditioned extracellular vesicles ($n = 7$) or saline (control, $n = 7$). Five weeks later, all animals underwent terminal harvest for perfusion measurements and myocardial sectioning.

Results: Myocardial perfusion analysis demonstrated a trend toward increase at rest and a significant increase during rapid pacing ($P = .09$, $P < .001$). There were significant increases in activated phosphorylated endothelial nitric oxide synthase, endothelial nitric oxide synthase, phosphatidylinositol 3-kinase, phosphorylated protein kinase B, and the phosphorylated protein kinase B/protein kinase B ratio in the hypoxia-conditioned extracellular vesicles group compared with the control group (all $P < .05$). Additionally, there was a significant decrease in the anti-angiogenic proteins collagen 18 and angiotatin ($P = .01$, $P = .01$) in the hypoxia-conditioned extracellular vesicles group.

Conclusions: Intramyocardial injection of hypoxia-conditioned extracellular vesicles results in increased myocardial perfusion without a corresponding change in vessel density. Therefore, this improvement in perfusion is possibly due to changes in nitric oxide signaling. Hypoxia-conditioned extracellular vesicles represent a potential therapeutic strategy to increase myocardial perfusion in patients with advanced coronary artery disease. (JTCVS Open 2024;20:49-63)



Ameroid constrictor placement.

CENTRAL MESSAGE

Intramyocardial injection of HEVs results in increased myocardial perfusion in a swine model of chronic myocardial ischemia.

PERSPECTIVE

Although there have been many advances in standard CAD therapeutics, patients with advanced CAD who are not eligible for endovascular stenting or surgical bypass have limited options. HEV treatment results in increased myocardial perfusion in our swine model, representing a potential therapeutic strategy in patients with advanced CAD.

From the Division of Cardiothoracic Surgery, Department of Surgery, Cardiovascular Research Center, Rhode Island Hospital, Alpert Medical School of Brown University, Providence, RI.

This research was funded by the National Institutes of Health T32HL160517 (M.B., D.D.H., C.S.); T32 GM065085 (C.X.); National Heart, Lung, and Blood Institute 1F32HL160063-01 (S.A.S.); R01HL133624 (M.R.A.); R56HL133624-05 (M.R.A.); a Rhode Island Foundation Grant 1472420231352 (M.R.A.); R01HL46716 (F.W.S.), and R01HL128831 (F.W.S.).

Institutional Review Board approval: All experiments were approved by the Institutional Animal Care and Use Committee of Rhode Island Hospital (Approval Number: 1791190-26, October 12, 2021).

Received for publication March 25, 2024; revisions received May 21, 2024; accepted for publication June 10, 2024; available ahead of print July 9, 2024.

Address for reprints: Frank W. Sellke, MD, FACS, Division of Cardiothoracic Surgery, Department of Surgery, Cardiovascular Research Center, Rhode Island Hospital, Alpert Medical School of Brown University, 2 Dudley St, MOC 360, Providence, RI 02905 (E-mail: fsellke@lifespan.org).


2666-2736

Copyright © 2024 The Author(s). Published by Elsevier Inc. on behalf of The American Association for Thoracic Surgery. This is an open access article under the CC BY-NC-ND license (<http://creativecommons.org/licenses/by-nc-nd/4.0/>).

<https://doi.org/10.1016/j.jtc.2024.06.003>

Abbreviations and Acronyms

AKT	= protein kinase B
CAD	= coronary artery disease
CON	= control
eNOS	= endothelial nitric oxide synthase
EV	= extracellular vesicle
HBMSC	= human bone marrow–derived stem cells
HEV	= hypoxia extracellular vesicles
LCx	= left circumflex coronary artery
p-AKT	= phosphorylated protein kinase B
p-eNOS	= phosphorylated endothelial nitric oxide synthase
PI3K	= phosphatidylinositol 3-kinase
TBST	= tris-buffered saline
TIMP-2	= tissue inhibitor of metalloproteinases 2

 Video clip is available online.

Coronary artery disease (CAD) is the leading cause of morbidity and mortality worldwide and a major contributor to hospital cost and total health system burden.^{1,2} Patients with advanced CAD who are not eligible for endovascular stenting or surgical bypass have limited options.^{3,4} This results in a significant subset of the population with end-stage, no-option disease.⁵ This group of patients often are placed on maximal medical therapy to prevent further ischemic injury. However, there is growing interest in technology that not only prevents further injury but also restores myocardial function.⁵ Extracellular vesicles (EVs) have emerged as a promising therapeutic modality to not only prevent further injury but also potentially restore myocardial function.⁶⁻⁸

EVs, which carry multiple types of cargo including lipids, proteins, and nucleic acids, are released into the extracellular environment and play a crucial role in cell-to-cell communication.^{9,10} EVs have shown potential in the treatment of multiple disease process, including trauma, limb ischemia, and ischemic cardiovascular disease.^{7,11-13} Our group has studied EVs derived from human bone marrow–derived mesenchymal stem cells (HBMSCs) extensively in our swine model of chronic myocardial ischemia.¹⁴⁻¹⁷ Using our model incorporating intramyocardial injection, we demonstrated several significant and clinically relevant improvements, including improved cardiac performance, augmented angiogenesis, and decreased inflammation.¹⁴⁻¹⁷

Although this work was conducted through the use of traditionally prepared EVs, it is possible to enhance the characteristics and therapeutic capabilities of EVs through additional environmental preconditioning.¹⁸⁻²¹ EVs are

conventionally developed using serum deprivation and in normal atmospheric oxygen levels; however, both oxygenation and growth media can be altered to influence ultimate EV phenotype.¹⁸ Hypoxia conditioning is especially noteworthy, because this modification may optimize EVs to function in the ischemic myocardium found in CAD. Additionally, our laboratory has shown using proteomic analysis that nonstarved hypoxia-conditioned extracellular vesicles (HEVs) express the largest and most diverse quantity of sub-proteins when compared with serum-starved HEVs, normoxic serum-starved EVs, and normoxic nonstarved EVs.¹⁸ We have previously published electron microscopy–generated morphologic data, immunoblotting, and proteomic data profiling of our HEVs.¹⁸

Given our prior success with standard EVs in conjunction with the benefits of hypoxia preconditioning, our laboratory has begun studying HEVs in a validated swine model of CAD. We have previously demonstrated that myocardial injection of HEVs results in reduced total apoptosis and that this change in apoptosis is likely related to increases in pro-survival pathways.²² We have further shown that HEVs resulted in alterations in inflammatory signaling and the myocardial response to oxidative stress.^{23,24} However, there was no change in studied functional parameters, including in cardiac output, ejection fraction, or systolic/diastolic ventricular function.²³ With nonconditioned EVs, we observed a significant increase in myocardial perfusion, and this was linked to increased myocardial angiogenesis.¹⁴ The goal of this study is to build on this body of work to enrich our understanding of the effects of HEVs on myocardial perfusion, angiogenesis, and nitric oxide signaling.

MATERIAL AND METHODS**Animal Model**

This study uses our previously published cohort of 14 Yorkshire swine (Cummings School of Veterinary Medicine of Tufts University Farm).^{22,23} All swine underwent left thoracotomy for placement of an ameroid constrictor (Research Instruments SW) on the left circumflex coronary artery (LCx). After the 2 weeks allotted for ameroid closure, swine underwent a redo left thoracotomy for intramyocardial injection of normal saline (CON, n = 7, male = 3, female = 4) or HEVs (n = 7, male = 3, female = 4).^{22,23} Five weeks after injection, swine underwent a terminal harvest procedure for perfusion measurement and tissue sectioning (Figure 1).

Animal Care

This protocol was approved by the Institutional Animal Care and Use Committee of Rhode Island Hospital (Approval Number: 1791190-26, 10/12/2021).^{22,23} All animals received humane care as previously reported and in compliance with the Principles of Laboratory Animal Care and the Guide for the Care and Use of Laboratory Animals.

Ameroid Placement

Swine received preoperative cephalexin (30 mg/kg) for antimicrobial prophylaxis and aspirin (10 mg/kg) orally 1 day preoperatively and

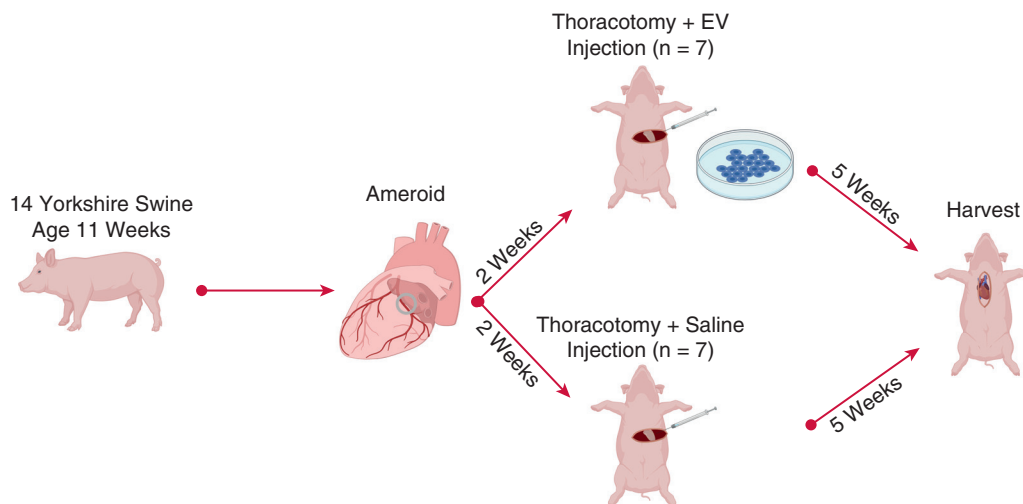


FIGURE 1. Methods. Fourteen Yorkshire swine underwent left thoracotomy for placement of an ameroid constrictor around the LCx. After 2 weeks of ischemic induction, swine underwent redo left thoracotomy with intramyocardial injection of normal saline ($n = 7$) or HEVs ($n = 7$). Five weeks after injection, all swine underwent a terminal harvest procedure with perfusion measurement and tissue sectioning. *EV*, Extracellular vesicle.

5 days postoperatively for thrombosis prophylaxis. Anesthesia was induced as previously reported with intramuscularly injected telazol (4.4 mg/kg) and xylazine (2.2 mg/kg).^{22,23} Swine were intubated, and general anesthesia was maintained using inhaled isoflurane. Swine were placed in a modified right lateral decubitus position with a slight tilt toward table left. Animals were prepped with betadine, and a left thoracotomy was performed through the second intercostal space. The pericardium was opened to expose the heart, whereupon the left atrial appendage was retracted to expose the LCx. Dissection of the LCx was carried back to its origin from the left main coronary artery. Swine were heparinized (80 IU/kg), and the LCx was encircled with a vessel loop. By using the vessel loop, the LCx was occluded for a duration of 2 minutes while simultaneously injecting 5 mL of gold microsphere solution (BioPal) into the right atrium to map the area at risk for ischemia. An ameroid constrictor was then placed at the base of the LCx as close to the left main coronary artery as possible to ensure creation of a uniform ischemic region across animals. The pericardium was then irrigated with saline to ensure hemostasis and subsequently closed with absorbable sutures. The chest was closed in layers using absorbable suture (Video 1). Postoperative pain control was the same as previously reported.²³

Extracellular Vesicle Culture

EV culture was conducted identically to our previously reported procedure.¹⁸ HBMSCs (Lonza) were cultivated in accordance with manufacturer's recommendations in growth medium (MSCGM Bulletkit PT-3001; Lonza) as previously described.¹⁸ Cells were cultured to passage 7 and 80% confluence. At this point, the culture medium was exchanged with fresh MSCGM media.¹⁸ Hypoxia was then induced in the cells through incubation in a humidified hypoxia chamber for 24 hours at 37 °C with an atmosphere composed of 5% carbon dioxide and 95% nitrogen.¹⁸ After 24 hours, media were collected, centrifuged, and extracted as previously described.¹⁸ HEVs were suspended in phosphate-buffered saline with 1% dimethyl sulfoxide and stored at -80°C .¹⁸ Protein quantification was performed with a Pierce BCA Protein Assay Kit (Thermo Fisher Scientific) to ensure a standardized quantity for injection.¹⁸

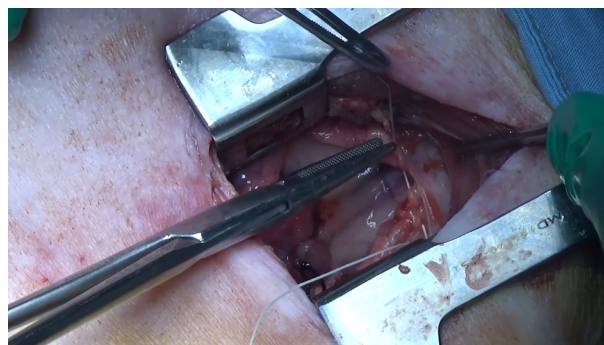
Extracellular Vesicle Proteomics

Proteomics was conducted on aliquots of HEVs in triplicate ($n = 3$).¹⁸ The samples were prepared and then run on liquid chromatography with tandem mass spectrometry as previously described.¹⁸ Peptide spectrum matching was searched against the UniProt protein database using the

Sequest algorithm with Proteome Discoverer v. 2.3 software (Thermo Fisher Scientific).¹⁸ Relative label-free quantitative analysis was then performed using the Minora algorithm. ShinyGO 0.76 (South Dakota State University) was used for pathway analysis.¹⁸

Extracellular Vesicle Injection

On the day of injection, HEVs (50 μg) were thawed and suspended in 2 mL of 0.9% sterile saline.²² According to our prior analysis, this 50 μg sample is composed of 2×10^9 HBMSC-EV particles.^{18,25} Anesthesia, preoperative antimicrobial prophylaxis, and preoperative thromboprophylaxis were the same as described in the "Ameroid Placement" section. The swine were again



VIDEO 1. Ameroid constrictor placement. A left thoracotomy was performed through the second intercostal space. The pericardium was opened to expose the heart. The left atrial appendage was retracted to expose the LCx. Dissection of the LCx was carried back to the origin from the left main coronary artery. The LCx was then encircled with a vessel loop. The LCx was occluded for a duration of 2 minutes while simultaneously injecting 5 mL solution of gold microspheres into the right atrium to map the area at risk for ischemia. An ameroid constrictor was then placed at the base of the LCx. The pericardium was irrigated with saline to ensure hemostasis and subsequently closed with absorbable sutures. The chest was closed in layers using absorbable sutures. *LCx*, Left circumflex coronary artery. Video available at: [https://www.jtcvs.org/article/S2666-2736\(24\)00161-X/fulltext](https://www.jtcvs.org/article/S2666-2736(24)00161-X/fulltext).

placed in a modified right lateral decubitus position with a slight tilt toward table left, prepped with betadine, and underwent left thoracotomy 1 intercostal space below the prior incision. Pulmonary adhesions were taken down as necessary with a combination of sharp and blunt dissection. The pericardium was reopened, and HEVs were injected into the myocardium in 10 locations adjacent to the LCx.²² The pericardium was irrigated with saline to ensure hemostasis and then closed with absorbable sutures, after which the chest was closed in layers using absorbable suture. Postoperative pain management was the same as described above in “Ameroid Placement.”

Harvest and Perfusion

Anesthesia and preoperative care were the same as described in “Ameroid Placement.” Swine were positioned supine and prepped with betadine. The chest was opened through a median sternotomy, and the pericardium was opened to expose the left atrium, right atrium, and apex.²³ A right groin cut-down was performed to access the right femoral artery. The Seldinger technique was used to place a 7F vascular sheath in the femoral artery, which was attached to a withdrawal pump (Harvard Apparatus). Labeled microspheres (BioPAL) were injected at rest and during rapid pacing at 150 beats per minute, while simultaneously withdrawing 10 mL of blood from the femoral artery to measure myocardial perfusion.²³ A pressure-volume catheter (Transonic) was advanced into the proximal aorta from the right femoral artery; a second pressure-volume catheter (Transonic) was then placed directly into left ventricle using the Seldinger technique.²³ After the completion of physiologic measurements, the animal was euthanized. The heart was removed and sectioned after removal based on the proximity of the tissue to the left anterior descending and LCx arteries. Segments were individually snap frozen in liquid nitrogen. Gold microsphere concentrations were used to identify the most and least ischemic areas, with the former most commonly originating from the free wall adjacent to the LCx.

Lysate Production

Lysates used in immunoblotting were produced from the ischemic and non-ischemic myocardial tissue of 7 experimental and 7 control animals. Myocardial tissue was lysed using the Halt Protease Inhibitor Cocktail (Thermo Fisher Scientific), RIPA Lysis and Extraction Buffer (Boston Bioproducts), and an ultrasonic homogenizer. Protein concentration was measured with the Pierce BCA Protein Assay Kit (Thermo Fisher Scientific).²²

Immunoblotting

A total of 40 μ g of protein lysate was run on a 4% to 12% Bis-Tris gel (Thermo Fisher Scientific) and then transferred onto a nitrocellulose membrane (Bio-Rad).²² Membranes were blocked in a 5% nonfat dry milk solution in tris-buffered saline (TBST, Boston BioProducts). Membranes were incubated with primary antibody dilutions in 5% bovine serum albumin in TBST for 24 hours (Table E1); washed with TBST and then incubated in horseradish-peroxidase-linked secondary antibody dilutions in 5% bovine serum albumin in TBST for 1 hour (Table E1); washed again with TBST and incubated with the Enhanced Chemiluminescence Western Blotting Substrate (Thermo Fisher Scientific) developing agent; and finally imaged on a ChemiDoc Imaging System (Bio-Rad).²² Repeat probing was conducted following use of Restore PLUS Western Blot Stripping Buffer (Thermo Fisher Scientific) as needed. Image J software version 1.54 (National Institutes of Health) was used to measure immunoblot band intensity.²³

Immunofluorescence

Arteriolar and capillary density were determined by immunofluorescent staining of frozen sections from ischemic myocardial tissue as previously described.²⁶ Frozen sections were thawed and fixed with 10% paraformaldehyde.²⁶ The slides were blocked in 3% bovine serum albumin in phosphate-buffered saline and incubated overnight in primary antibody to α -smooth muscle actin or isolectin B4 (Table E1).²⁶ Slides were then rinsed with phosphate-buffered saline and incubated with secondary antibody for

1 hour.²⁶ Slides were rinsed again and incubated in DAPI for 5 minutes and then mounted for imaging using an Olympus VS200 Slide Scanner (Olympus Corporation). QuPath software 5.0 was used for image analysis, with capillary density determined by percent of tissue area stained with isolectin B4, and arteriolar count determined by counting the number of smooth muscle actin-staining objects with a minimum size of 100 μ m² per area of tissue sections.²⁷

Statistics

Prism 10 (GraphPad Software) was used for data analysis. The Shapiro-Wilk test was used to determine normality, and data that followed a normal distribution were analyzed with the Student *t* test, and nonparametric data were analyzed with the Mann-Whitney *U* test. Immunoblot data are represented as mean fold change normalized to the control group average as previously described. Protein expression was correlated to myocardial perfusion using the Spearman rank correlation. Outliers greater than 2 SDs from the mean were excluded from analysis.

RESULTS

Hypoxia-Conditioned Extracellular Vesicle Proteomics

We have previously demonstrated the absence of albumin and the presence of the transmembrane proteins CD81 and CD91 in HEVs using immunoblotting.¹⁸ HEVs were previously evaluated with electron microscopy and found to have a mean particle size of 179.2 \pm 7.3 nm.¹⁸ Proteomic analysis of HEVs identified 395 unique proteins, as previously reported by our group. This included 15 proteins involved in angiogenesis and AKT signaling (Table 1).

Hypoxia-Conditioned Extracellular Vesicles Improve Myocardial Perfusion

Myocardial perfusion analysis showed a trend toward increased myocardial perfusion at rest and a significant

TABLE 1. Protein kinase B signaling and angiogenesis proteomics

Protein name	Log ₁₀ (abundance)
14-3-3 Protein	7.2 (7.1-7.2)
Alpha-actinin-4	6.5 (6.5-6.6)
Cadherin-13	6.1 (6.0-6.1)
Fibronectin	7.7 (7.7-7.8)
GTPase KRAS	5.9 (5.9-5.9)
GTP binding protein	6.0 (6.0-6.0)
Guanine nucleotide-binding protein	7.1 (7.0-7.1)
Heat shock protein 90	6.6 (6.6-6.7)
Integrin-alpha	5.8 (5.8-5.8)
Integrin-beta	7.8 (7.7-7.8)
Junction plakoglobin	5.0 (4.9-5.1)
Myosin heavy polypeptide 9	5.9 (5.8-5.9)
Ras homolog	6.3 (6.3-6.3)
Thrombospondin-1	6.5 (6.5-6.5)
Tyrosine 3-monooxygenase	5.5 (5.4-5.5)

The proteins identified in the HEV proteomics that contribute to angiogenesis and AKT signaling. Data are displayed as the Log₁₀ of the average protein abundance from the 3 samples used in this experiment along with the min and max Log₁₀ of protein abundance in parentheses. HEV, Hypoxia extracellular vesicles; AKT, protein kinase B.

increase in ischemic myocardial perfusion while pacing the heart at 150 bpm in the HEV group when compared with the CON group ($P = .09$, $P < .001$, Figure 2, A, Table E2).

Hypoxia-Conditioned Extracellular Vesicles Do Not Change Myocardial Vascular Density

No changes were observed in arteriolar density by α -smooth muscle actin or capillary density by isolectin B4 in the ischemic myocardium between the HEV and CON

groups ($P = .56$ and $P = .14$, respectively, Figure 2, B, Table E2).

Hypoxia-Conditioned Extracellular Vesicles Modulate Angiogenic Signaling

There was a significant decrease in antiangiogenic proteins collagen 18 and angiostatin in ischemic myocardial lysates from the HEV group ($P = .01$ and $P = .01$, respectively, Figure 2). This tissue also exhibited a

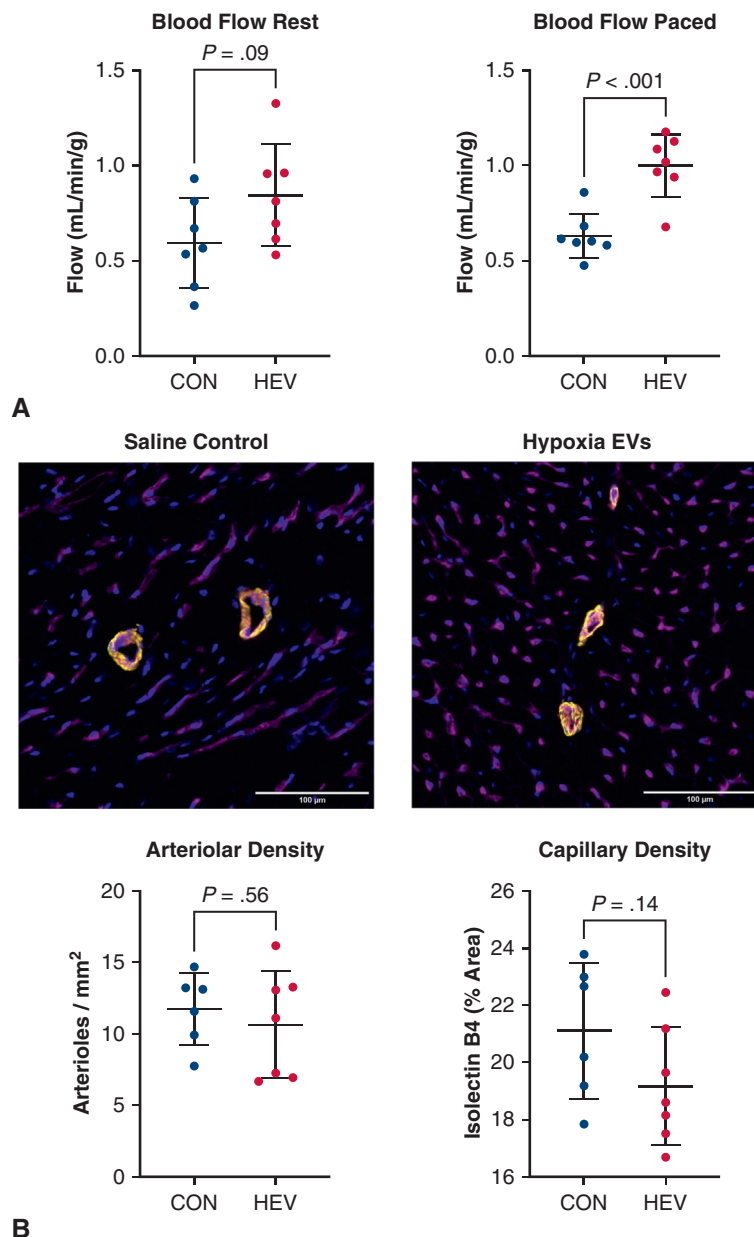


FIGURE 2. Myocardial perfusion and vascular density. A, Myocardial perfusion analysis showed a trend toward increased myocardial perfusion at rest and a significant increase in myocardial perfusion while pacing the heart at 150 bpm in the HEV group compared with the CON group. B, No changes were observed in arteriolar density by α -smooth muscle actin (yellow) or capillary density by isolectin B4 (magenta) between the HEV and CON groups. The DAPI nuclear stain appears in blue. CON, Control; HEV, hypoxia extracellular vesicle; EV, extracellular vesicle.

significant increase in the antiangiogenic mediators tissue inhibitor of metalloproteinases 2 (TIMP-2), plasminogen, and cathepsin B compared with the CON group (all $P < .05$, Figure 2). There was no significant change in cathepsin D, cathepsin L, and endostatin (all $P > .05$, Figure 3, Table E2).

Hypoxia-Conditioned Extracellular Vesicles Augment Nitric Oxide Signaling

There were significant increases in phosphorylated-endothelial nitric oxide synthase (p-eNOS), endothelial nitric oxide synthase (eNOS), phosphatidylinositol 3-kinase (PI3K), phosphorylated-protein kinase B (p-AKT), protein

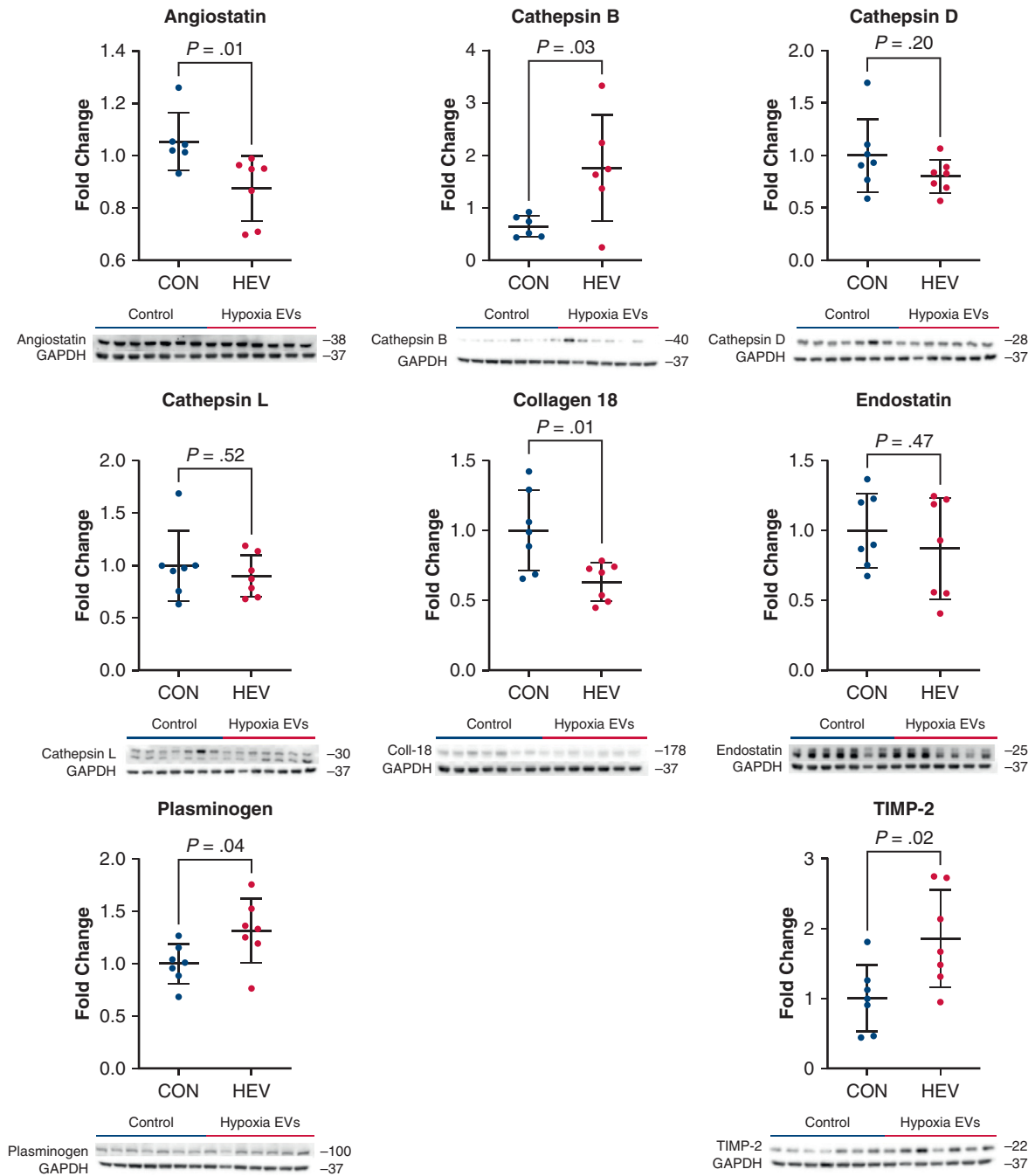


FIGURE 3. Angiogenic signaling. There was a significant decrease in antiangiogenic collagen 18 and angiostatin in the HEV group compared with the CON group. The HEV group also exhibited a significant increase in antiangiogenic TIMP-2, plasminogen, and cathepsin B compared with CON. There was no significant change in cathepsin D, cathepsin L, endostatin, and Tie 2. Immunoblot data are represented as mean fold change normalized to the CON mean as previously described. All data are represented as mean plus or minus SD. CON, Control; HEV, hypoxia extracellular vesicle; TIMP-2, tissue inhibitor of metalloproteinases 2; EV, extracellular vesicle.

kinase B (AKT), and the ratio of p-AKT to AKT in the ischemic myocardium of the HEV group when compared with CON (all $P < .05$, Figure 4, Table E2).

Myocardial Perfusion Is Correlated With Protein Expression

There was a significant positive correlation with ischemic myocardial perfusion during pacing and protein expression of p-eNOS, eNOS, TIMP-2, and PI3K (all

$P < .05$, Table 2). There was a significant negative correlation with ischemic myocardial perfusion during pacing and protein expression of collagen 18 and angiostatin ($P = .02$, $P = .008$, Table 2). There was no significant correlation with perfusion at rest and any of the tested proteins (all $P > .05$, Table 2). There was no significant correlation with ischemic myocardial perfusion while pacing with AKT, p-AKT, and cathepsin B (all $P > .05$, Table 2, Table E2).

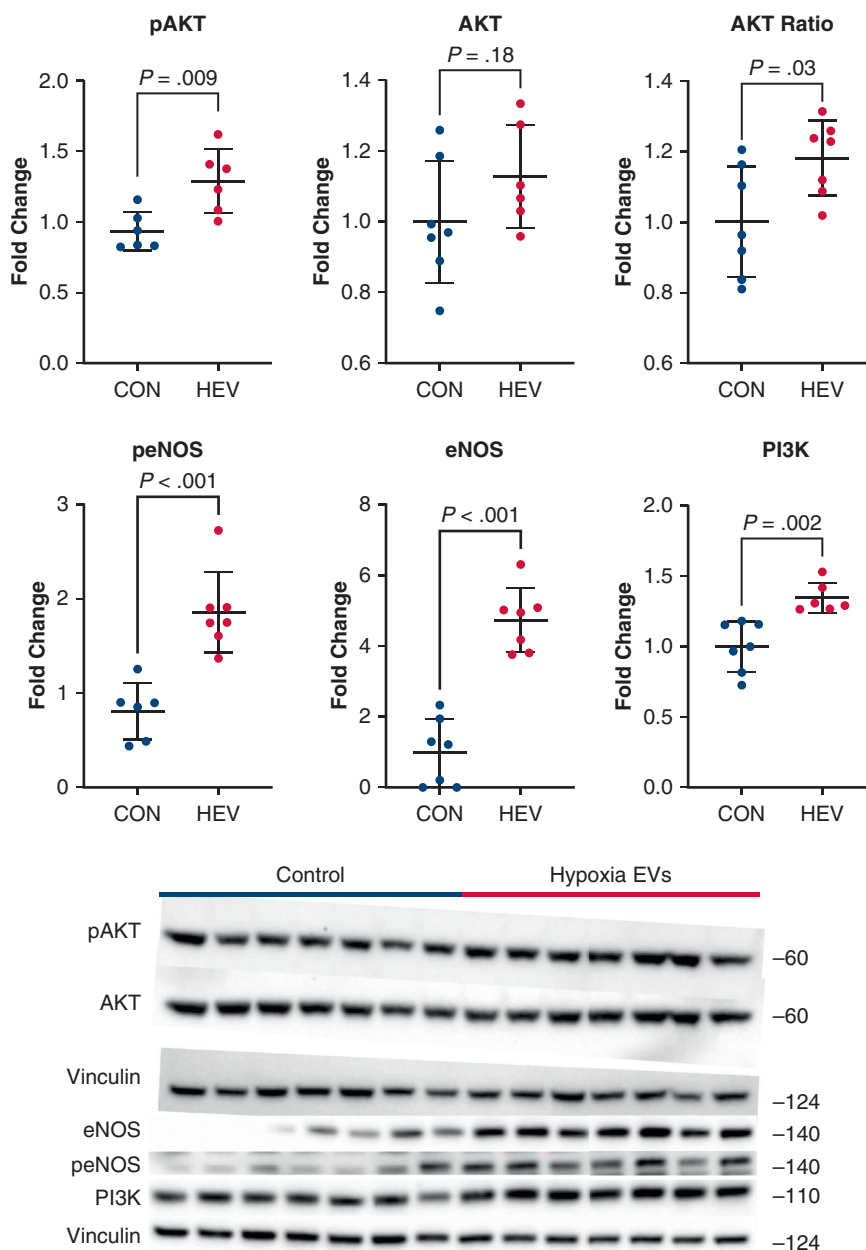


FIGURE 4. Nitric oxide signaling. There were significant increases in p-eNOS, the p-eNOS to eNOS ratio, PI3K, p-AKT, AKT, and the ratio of p-AKT to AKT in the HEV group compared with CON. There was a trend toward decreased eNOS in the HEV group compared with CON. Immunoblot data are represented as mean fold change normalized to the CON mean as previously described. All data are represented as mean plus or minus SD. *p-AKT*, Phosphorylated protein kinase B; *CON*, control; *HEV*, hypoxia extracellular vesicles; *AKT*, protein kinase B; *p-eNOS*, phosphorylated endothelial nitric oxide synthase; *eNOS*, endothelial nitric oxide synthase; *PI3K*, phosphatidylinositol 3-kinase; *EV*, extracellular vesicle.

TABLE 2. Perfusion correlation

Protein	Rest		Paced	
	r	P	r	P
AKT	0.15	.62	0.27	.37
p-AKT	0.22	.49	0.49	.11
Angiostatin	0.24	.43	−0.69	.008
Cathepsin B	0.08	.36	0.20	.15
Collagen 18	−0.19	.51	−0.63	.02
p-eNOS	−0.40	.17	0.75	.003
eNOS	−0.24	.40	0.92	< .001
PI3K	−0.40	.16	0.95	< .001
Plasminogen	0.09	.30	0.63	.02
TIMP-2	0.19	.12	0.56	.04

The correlation (r) between myocardial perfusion and protein expression. Significant probability values are in bold. *AKT*, Protein kinase B; *p-AKT*, phosphorylated protein kinase B; *p-eNOS*, phosphorylated endothelial nitric oxide synthase; *eNOS*, endothelial nitric oxide synthase; *PI3K*, phosphatidylinositol 3-kinase; *TIMP-2*, tissue inhibitor of metalloproteinases 2.

Hypoxia-Conditioned Extracellular Vesicles Produce Minimal Changes in the Nonischemic Myocardium

There was no difference in nonischemic myocardial perfusion at rest or while pacing the heart at 150 bpm between the HEV and CON groups ($P = .66$, $P = .66$, Figure E1, A). There was no difference in expression of collagen 18, angiostatin, plasminogen, TIMP-2, cathepsin B, p-eNOS, eNOS, AKT, or p-AKT in nonischemic HEV myocardium compared with CON (all $P > .05$, Figure E1, B, Figure E2). There was a significant increase in PI3K in the nonischemic HEV myocardium compared with CON ($P < .001$, Figure E2, Table E2).

DISCUSSION

Despite the multitude of therapeutic advances for patients with CAD, patients with advanced disease who are not eligible for revascularization have limited options.³ There is growing interest in EVs as a novel modality capable of not only preventing further injury but also restoring previously lost myocardial function. Given this growing interest and the corresponding need to cultivate a product with maximal translational potential, we have developed HEVs with the hope they will be optimized to function within the hypoxic context of ischemic myocardial disease. We have previously shown that HEVs express the greatest diversity of sub-proteins when compared with alternative methods of EV conditioning.¹⁸ In this analysis, we expanded our characterization of HEV-associated protein content through identification of 15 markers that are involved in AKT signaling and angiogenesis.

In addition to marker analysis, our blood flow assays showed that the ischemic myocardium of the HEV group exhibited a significant increase in myocardial perfusion during rapid ventricular pacing, as well as a strong trend toward

increased myocardial perfusion at rest. This increase in perfusion was not related to an increase capillary or arteriolar density, but was accompanied by multiple notable protein expression changes elicited by immunoblotting of ischemic myocardium. First, there was a combination of both decreased expression of the antiangiogenic proteins collagen 18 and angiostatin, and increased expression of anti-angiogenic TIMP-2 and cathepsin B.²⁸⁻³¹ The increase in plasminogen we also observed may reflect decreased breakdown of plasminogen into angiostatin.³² These findings are noteworthy not only for the account of molecular correlates of increased perfusion that they provide but also for the lack of correlation they exhibit between myocardial angiogenesis. The lack of microvascular changes we observed suggests that the changes in perfusion are related to changes in ischemic myocardium microvascular reactivity, rather than to total vascular count.

This contention is supported by the modulation we also showed of several proteins involved in vascular reactivity in the ischemic myocardium. Specifically, the HEV group exhibited a significant increase in vasodilatory p-eNOS, as well as total eNOS.^{33,34} This may be related to an increase in the upstream signaling mediators p-AKT and PI3K; this interaction is further validated by a significant positive trend between p-eNOS, eNOS, and PI3K expression and perfusion of the ischemic myocardium, as well as by the multiple upregulated proteins related to PI3K/AKT signaling found previously through proteomic profiling of HEVs.³⁵ Conversely, we observed decreases in the vasoconstrictive proteins collagen 18 and angiostatin, along with a significant negative trend between expression of these proteins and myocardial perfusion.^{28,36} Taken together, these findings suggest changes in vascular reactivity related to both increases in vasodilatory proteins and decreases in vasoconstrictive counterparts as an account of the augmented

perfusion observed in our study. This change in perfusion is most notable with pacing, implying that the increase in perfusion and release of nitric oxide are potentially related to a myocardial stress response. The tissue collected in the study was only collected after pacing the heart, however, precluding comparison between stressed and unstressed tissue in this study. Patients with refractory angina often experience symptoms with mild to moderate stress,³⁷ positioning this increase in perfusion with myocardial stress as a clinically relevant consequence of HEV administration in patients with refractory angina.

The results of this study differ from our previous results using traditional, nonhypoxia-conditioned EVs.¹⁴ In this previous work, EV treatment resulted in increased myocardial perfusion; however, the increase in perfusion was correlated with increases in arteriolar and capillary density.¹⁴ The results of our previous study also showed increased nitric oxide and AKT signaling similar to the current study.¹⁴ These differences suggest that HEVs result in changes in vascular reactivity, as opposed to the increased angiogenesis seen with traditional EVs. A study comparing HEVs with traditional EVs is necessary to further understand this difference and any functional implications it may confer.

Finally, EV-injected tissue in the nonischemic area did not produce a significant change in myocardial perfusion or protein expression, apart from in PI3K. This suggests that HEVs have minimal impact on the surrounding healthy tissue.

Our results demonstrate that HEVs produce a significant increase in myocardial perfusion independent of myocardial neovascularization and likely related to favorable alterations in microvascular reactivity. Taken together with our

previously described decreases in myocardial apoptosis, modulation of oxidative stress, and decreased cardiac inflammation, this study indicates that HEVs may induce pleiotropic tissue-level benefits for patients with advanced ischemic myocardial disease (Figure 5).²²⁻²⁴ Further studies are needed to delineate the optimal type of EVs for use in human studies; the results of our study suggest that follow-up experiments designed to evaluate the effects of HEVs in conjunction with revascularization in anticipation of future human studies are warranted.

Study Limitations

Although these results substantially expand our mechanistic understanding of the potential held by HEV therapy to augment perfusion to the ischemic myocardium in CAD, their accurate interpretation requires consideration of several limitations. First, the sample size of 7 animals per group could result in inadequate power to identify small changes in myocardial function or protein signaling. We have previously found changes in perfusion and angiogenesis with EVs using sample sizes of 8 to 10,^{14,17,38} but the slightly lower size of the current cohort likely limits the power of this study. Likewise, our study used a mixed cohort with respect to sex, but is underpowered to conduct sex-specific analysis given its small sample size. Additionally, our methodology permits evaluation of only 1 dose of injection and 1 time point, whereas findings could be impacted by different doses, additional time points, or different analytic durations. The lack of the ability to perform microvascular studies at the time of this experiment prevented inclusion in our dataset of additional corroborating evidence of the dependence of perfusion changes on vascular reactivity. Finally, EV studies in general are limited by

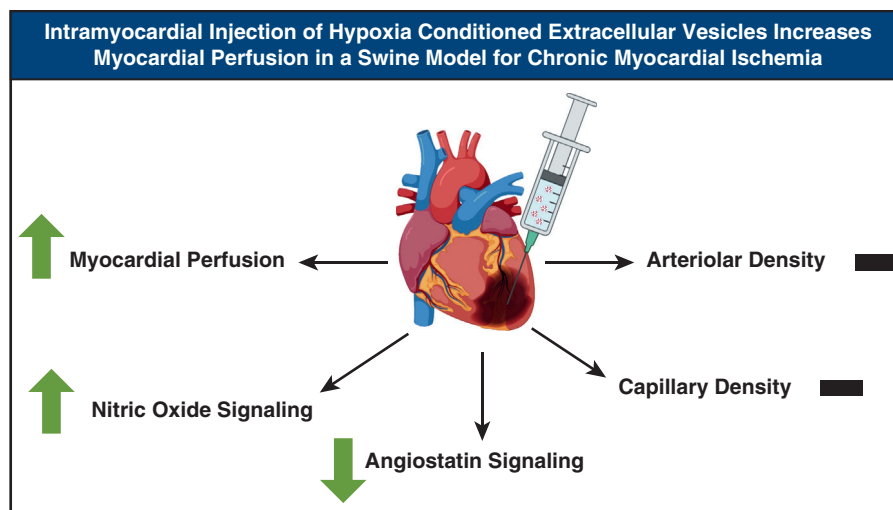


FIGURE 5. Graphical Abstract. Intramyocardial injection of HEVs results in increased myocardial perfusion without a corresponding change in myocardial vascular density. This suggests modulation of vasodilatory nitric oxide signaling, as well as of vasoconstrictive mediators, may be responsible for the observed change in perfusion.

the reproducibility of EVs between laboratories. It has been shown that different laboratories can use the same cell lines and similar culture methods, and nevertheless produce different EVs.³⁹ This is a well-recognized issue among EV researchers that requires further standardization in anticipation of large-scale production. This, in turn, requires specification of the optimal conditioning protocol, and we hope our results will contribute to this effort.³⁹

CONCLUSIONS

Intramyocardial injection of HEVs results in increased myocardial perfusion, particularly in the setting of myocardial stress, and without a corresponding change in myocardial vascular density. This suggests that modulation of the vasodilatory protein p-eNOS, as well as of the vasoconstrictive mediators collagen 18 and angiotensin, may account for the observed change in perfusion through corresponding modulation of microvascular reactivity. These results position HEV treatment as a potential therapeutic strategy to increase myocardial perfusion in patients with advanced CAD.

Conflict of Interest Statement

The authors reported no conflicts of interest.

The *Journal* policy requires editors and reviewers to disclose conflicts of interest and to decline handling or reviewing manuscripts for which they may have a conflict of interest. The editors and reviewers of this article have no conflicts of interest.

The authors thank the veterinary and animal care staff at Rhode Island Hospital.

References

- Lindstrom M, DeCleene N, Dorsey H, et al. Global burden of cardiovascular diseases and risks collaboration, 1990-2021. *J Am Coll Cardiol*. 2022;80(25):2372-2425. <https://doi.org/10.1016/j.jacc.2022.11.001>
- Tsao CW, Aday AW, Almarzooq ZI, et al. Heart disease and stroke statistics-2022 update: a report from the American Heart Association. *Circulation*. 2022;145(8):e153-e639. <https://doi.org/10.1161/CIR.0000000000001052>
- Lassaletta AD, Chu LM, Sellke FW. Therapeutic neovascularization for coronary disease: current state and future prospects. *Basic Res Cardiol*. 2011;106(6):897-909. <https://doi.org/10.1007/s00395-011-0200-1>
- Knuuti J, Wijns W, Saraste A, et al. 2019 ESC guidelines for the diagnosis and management of chronic coronary syndromes. *Eur Heart J*. 2020;41(3):407-477. <https://doi.org/10.1093/eurheartj/ehz425>
- Manfredi R, Verdoia M, Compagnucci P, et al. Angina in 2022: current perspectives. *J Clin Med*. 2022;11(23):6891. <https://doi.org/10.3390/jcm11236891>
- Kandaswamy E, Zuo L. Recent advances in treatment of coronary artery disease: role of science and technology. *Int J Mol Sci*. 2018;19(2):424. <https://doi.org/10.3390/ijms19020424>
- Fu S, Zhang Y, Li Y, Luo L, Zhao Y, Yao Y. Extracellular vesicles in cardiovascular diseases. *Cell Death Discov*. 2020;6:68. <https://doi.org/10.1038/s41420-020-00305-y>
- Karbasiafshar C, Sellke FW, Abid MR. Mesenchymal stem cell-derived extracellular vesicles in the failing heart: past, present, and future. *Am J Physiol Heart Circ Physiol*. 2021;320(5):H1999-H2010. <https://doi.org/10.1152/ajpheart.00951.2020>
- Alibhai FJ, Tobin SW, Yeganeh A, Weisel RD, Li RK. Emerging roles of extracellular vesicles in cardiac repair and rejuvenation. *Am J Physiol Heart Circ Physiol*. 2018;315(4):H733-H744. <https://doi.org/10.1152/ajpheart.00100.2018>
- Jeppesen DK, Fenix AM, Franklin JL, et al. Reassessment of exosome composition. *Cell*. 2019;177(2):428-445.e18. <https://doi.org/10.1016/j.cell.2019.02.029>
- Mathieu M, Martin-Jaular L, Lavieu G, Théry C. Specificities of secretion and uptake of exosomes and other extracellular vesicles for cell-to-cell communication. *Nat Cell Biol*. 2019;21(1):9-17. <https://doi.org/10.1038/s41556-018-0250-9>
- Alsaadi N, Srinivasan AJ, Seshadri A, Shiel M, Neal MD, Scott MJ. The emerging therapeutic potential of extracellular vesicles in trauma. *J Leukoc Biol*. 2022;111(1):93-111. <https://doi.org/10.1002/JLB.3MIR0621-298R>
- Cavallari C, Ranghino A, Tapparo M, et al. Serum-derived extracellular vesicles (EVs) impact on vascular remodeling and prevent muscle damage in acute hind limb ischemia. *Sci Rep*. 2017;7(1):8180. <https://doi.org/10.1038/s41598-017-08250-0>
- Reed SL, Escayg A. Extracellular vesicles in the treatment of neurological disorders. *Neurobiol Dis*. 2021;157:105445. <https://doi.org/10.1016/j.nbd.2021.105445>
- Potz BA, Scrimgeour LA, Pavlov VI, Sodha NR, Abid MR, Sellke FW. Extracellular vesicle injection improves myocardial function and increases angiogenesis in a swine model of chronic ischemia. *J Am Heart Assoc*. 2018;7(12):e008344. <https://doi.org/10.1161/JAHA.117.008344>
- Broadwin M, Aghagholi G, Sabe SA, et al. Extracellular vesicle treatment partially reverts epigenetic alterations in chronically ischemic porcine myocardium. *Vessel Plus*. 2023;7:25. <https://doi.org/10.20517/2574-1209.2023.103>
- Sabe SA, Scrimgeour LA, Karbasiafshar C, et al. Extracellular vesicles modulate inflammatory signaling in chronically ischemic myocardium of swine with metabolic syndrome. *J Thorac Cardiovasc Surg*. 2023;165(5):e225-e236. <https://doi.org/10.1016/j.jtcvs.2022.07.016>
- Scrimgeour LA, Potz BA, Aboul Gheit A, et al. Extracellular vesicles promote arteriogenesis in chronically ischemic myocardium in the setting of metabolic syndrome. *J Am Heart Assoc*. 2019;8(15):e012617. <https://doi.org/10.1161/JAHA.119.012617>
- Xu CM, Karbasiafshar C, Brinck Teixeira R, et al. Proteomic assessment of hypoxia-pre-conditioned human bone marrow mesenchymal stem cell-derived extracellular vesicles demonstrates promise in the treatment of cardiovascular disease. *Int J Mol Sci*. 2023;24(2):1674. <https://doi.org/10.3390/ijms24021674>
- Pulido-Escribano V, Torrecillas-Baena B, Camacho-Cardenosa M, Dorado G, Gálvez-Moreno MÁ, Casado-Díaz A. Role of hypoxia preconditioning in therapeutic potential of mesenchymal stem-cell-derived extracellular vesicles. *World J Stem Cells*. 2022;14(7):453-472. <https://doi.org/10.4252/wjsc.v14.i7.453>
- Zhu J, Lu K, Zhang N, et al. Myocardial reparative functions of exosomes from mesenchymal stem cells are enhanced by hypoxia treatment of the cells via transferring microRNA-210 in an nSMase2-dependent way. *Artif Cells Nanomedicine Biotechnol*. 2018;46(8):1659-1670. <https://doi.org/10.1080/21691401.2017.1388249>
- Mao CY, Zhang TT, Li DJ, et al. Extracellular vesicles from hypoxia-preconditioned mesenchymal stem cells alleviates myocardial injury by targeting thioredoxin-interacting protein-mediated hypoxia-inducible factor-1 α pathway. *World J Stem Cells*. 2022;14(2):183-199. <https://doi.org/10.4252/wjsc.v14.i2.183>
- Harris DD, Sabe SA, Sabra M, et al. Intramyocardial injection of hypoxia-conditioned extracellular vesicles modulates apoptotic signaling in chronically ischemic myocardium. *JTCVS Open*. 2023;15:220-228. <https://doi.org/10.1016/j.xjon.2023.05.013>
- Harris DD, Sabe SA, Broadwin M, et al. Intramyocardial injection of hypoxia-conditioned extracellular vesicles modulates response to oxidative stress in the chronically ischemic myocardium. *Bioengineering (Basel)*. 2024;11(2):125. <https://doi.org/10.3390/bioengineering11020125>
- Sabra M, Sabe SA, Harris DD, et al. Ischemic myocardial inflammatory signaling in starvation versus hypoxia-derived extracellular vesicles: a comparative analysis. *JTCVS Open*. 2023;16:419-428. <https://doi.org/10.1016/j.xjon.2023.10.004>
- Xu CM, Sabe SA, Brinck-Teixeira R, Sabra M, Sellke FW, Abid MR. Visualization of cardiac uptake of bone marrow mesenchymal stem cell-derived extracellular vesicles after intramyocardial or intravenous injection in murine myocardial infarction. *Physiol Rep*. 2023;11(6):e15568. <https://doi.org/10.14814/phy2.15568>
- Sabe SA, Xu CM, Sabra M, et al. Canagliflozin improves myocardial perfusion, fibrosis, and function in a swine model of chronic myocardial ischemia. *J Am Heart Assoc*. 2023;12(1):e028623. <https://doi.org/10.1161/JAHA.122.028623>

28. Bankhead P, Loughrey MB, Fernández JA, et al. QuPath: open source software for digital pathology image analysis. *Sci Rep*. 2017;7(1):16878. <https://doi.org/10.1038/s41598-017-17204-5>
29. Moulton KS, Olsen BR, Sonn S, Fukai N, Zurakowski D, Zeng X. Loss of collagen XVIII enhances neovascularization and vascular permeability in atherosclerosis. *Circulation*. 2004;110(10):1330-1336. <https://doi.org/10.1161/01.CIR.0000140720.79015.3C>
30. O'Reilly MS, Holmgren L, Shing Y, et al. Angiostatin: a novel angiogenesis inhibitor that mediates the suppression of metastases by a Lewis lung carcinoma. *Cell*. 1994;79(2):315-328. [https://doi.org/10.1016/0092-8674\(94\)90200-3](https://doi.org/10.1016/0092-8674(94)90200-3)
31. Stetler-Stevenson WG, Seo DW. TIMP-2: an endogenous inhibitor of angiogenesis. *Trends Mol Med*. 2005;11(3):97-103. <https://doi.org/10.1016/j.molmed.2005.01.007>
32. Im E, Venkatakrisnan A, Kazlauskas A. Cathepsin B regulates the intrinsic angiogenic threshold of endothelial cells. *Mol Biol Cell*. 2005;16(8):3488-3500. <https://doi.org/10.1091/mbc.E04-11-1029>
33. Gately S, Twardowski P, Stack MS, et al. The mechanism of cancer-mediated conversion of plasminogen to the angiogenesis inhibitor angiostatin. *Proc Natl Acad Sci U S A*. 1997;94(20):10868. <https://doi.org/10.1073/pnas.94.20.10868>
34. Kukreja RC, Xi L. eNOS phosphorylation: a pivotal molecular switch in vasodilation and cardioprotection? *J Mol Cell Cardiol*. 2007;42(2):280-282. <https://doi.org/10.1016/j.yjmcc.2006.10.011>
35. Tran N, Garcia T, Aniq M, Ali S, Ally A, Nauli S. Endothelial nitric oxide synthase (eNOS) and the cardiovascular system: in physiology and in disease states. *Am J Biomed Sci Res*. 2022;15(2):153-177.
36. Lee MY, Luciano AK, Ackah E, et al. Endothelial Akt1 mediates angiogenesis by phosphorylating multiple angiogenic substrates. *Proc Natl Acad Sci*. 2014; 111(35):12865-12870. <https://doi.org/10.1073/pnas.1408472111>
37. Koshida R, Ou J, Matsunaga T, et al. Angiostatin: a negative regulator of endothelial-dependent vasodilation. *Circulation*. 2003;107(6):803-806. <https://doi.org/10.1161/01.CIR.0000057551.88851.09>
38. Scrimgeour LA, Potz BA, Aboul Gheit A, et al. Intravenous injection of extracellular vesicles to treat chronic myocardial ischemia. *PLoS One*. 2020; 15(9):e0238879. <https://doi.org/10.1371/journal.pone.0238879>
39. Li G, Chen T, Dahlman J, et al. Current challenges and future directions for engineering extracellular vesicles for heart, lung, blood and sleep diseases. *J Extracell Vesicles*. 2023;12(2):12305. <https://doi.org/10.1002/jev2.12305>

Key Words: chronic myocardial ischemia, extracellular vesicles, hypoxia conditioned, intramyocardial injection, myocardial perfusion, swine

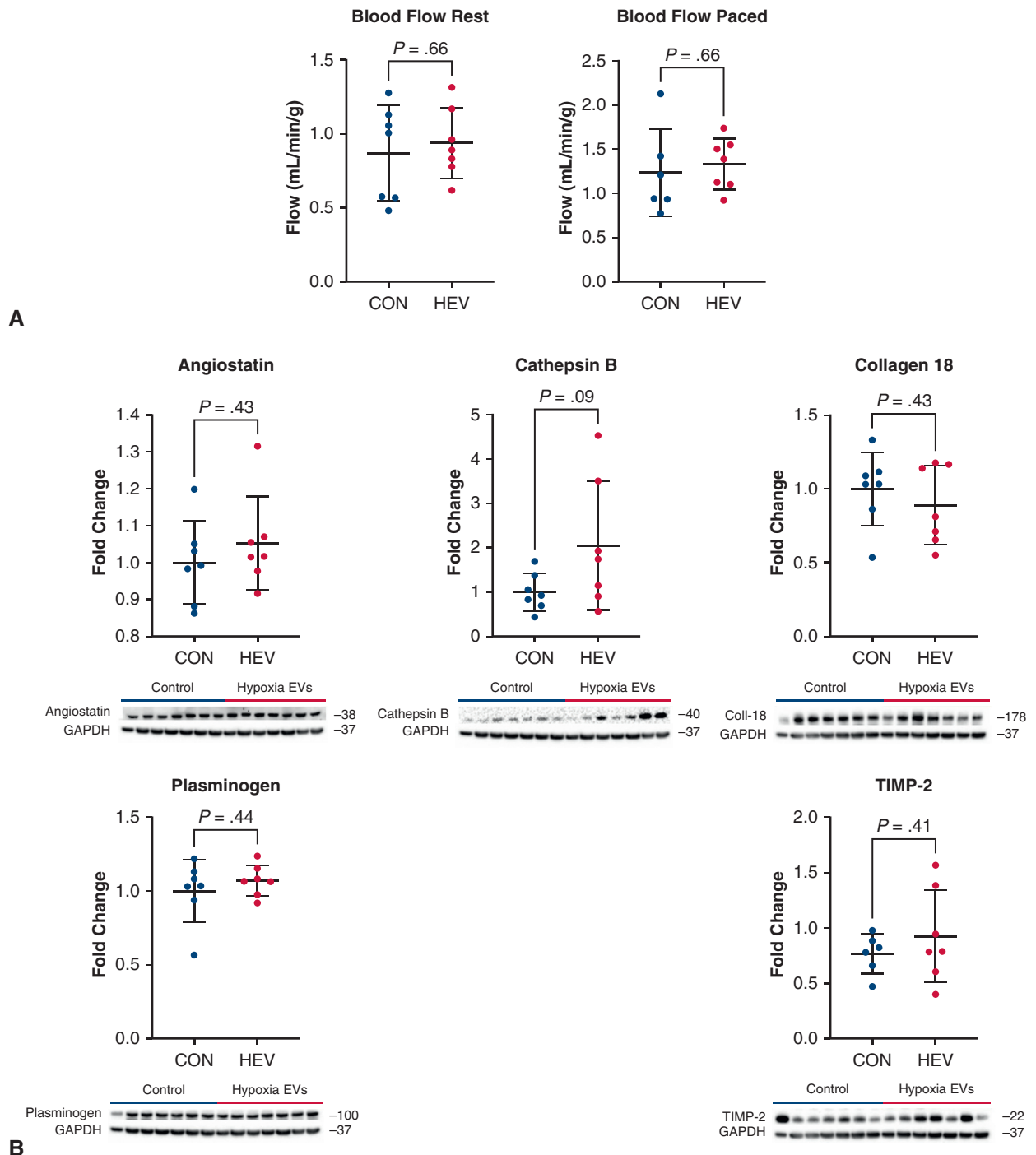


FIGURE E1. Nonischemic perfusion and angiogenic signaling. A, There was no difference in nonischemic myocardial perfusion at rest or while pacing the heart at 150 bpm between the HEV group compared with the CON group. B, There was no difference in expression of collagen 18, angiostatin, plasminogen, TIMP-2, or cathepsin B. Immunoblot data are represented as mean fold change normalized to the average control. All data are represented as mean plus or minus SD. CON, Control; HEV, hypoxia extracellular vesicle; TIMP-2, tissue inhibitor of metalloproteinases 2.

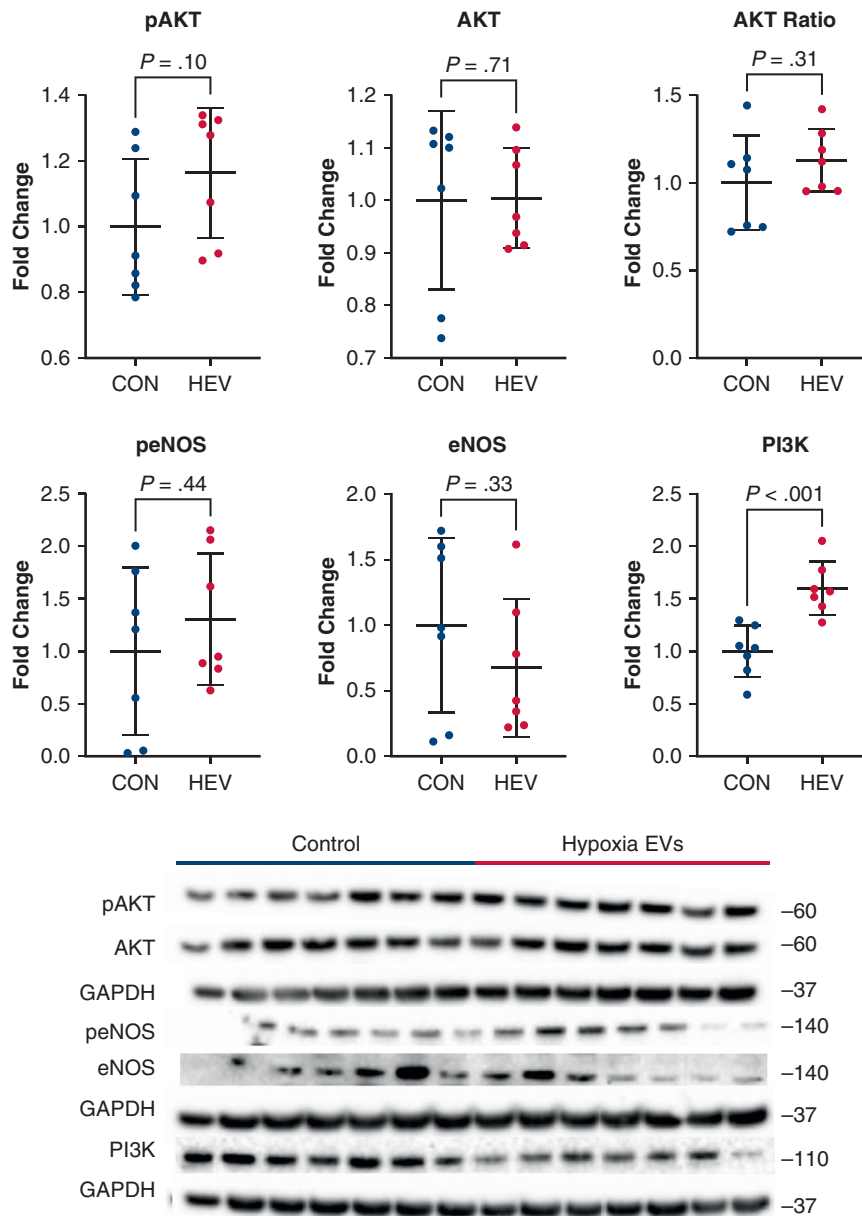


FIGURE E2. Nonischemic nitric oxide signaling. There was no difference in nonischemic myocardial expression of p-eNOS, eNOS, p-AKT, AKT, or the ratio of p-AKT to AKT in the HEV group compared with CON. There was a significant increase in PI3K in the HEV group compared to CON. Immunoblot data are represented as mean fold change normalized to the CON mean. All data are represented as mean plus or minus SD. *p-AKT*, Phosphorylated protein kinase B; *CON*, control; *HEV*, hypoxia extracellular vesicle; *AKT*, protein kinase B; *p-eNOS*, phosphorylated endothelial nitric oxide synthase; *eNOS*, endothelial nitric oxide synthase; *PI3K*, phosphatidylinositol 3-kinase; *EV*, extracellular vesicle.

TABLE E1. Antibodies

Antibody	Company	Catalog no.
Primary antibodies		
Alpha-smooth muscle actin	Abcam	7817
Angiostatin/plasminogen	Abcam	2904
Cathepsin B	Cell Signaling	3178
Cathepsin D	Cell Signaling	69854
Cathepsin L	Cell Signaling	71298
Collagen 18/endostatin	Abcam	275390
Phosphorylated-endothelial nitric oxide synthase	Cell Signaling	9571
Endothelial nitric oxide synthase	Cell Signaling	32027
Isolectin B4	Thermo Fisher Scientific	132450
Phosphatidylinositol 3-kinases	Cell Signaling	4249
Phosphorylated-protein kinase B	Cell Signaling	4060
Protein kinase B	Cell Signaling	9272
Tissue inhibitor of metalloproteinases 2	Cell Signaling	5738
Secondary antibodies		
Anti-mouse HRP-linked antibody	Cell Signaling	7076S
Anti-rabbit HRP-linked antibody	Cell Signaling	7074S
Anti-mouse Alexa Fluor 594	Cell Signaling	8890

The antibodies used in the experiment, along with manufacturers and catalog numbers. *HRP*, Horseradish peroxidase.

TABLE E2. Data

	Control	Hypoxia extracellular vesicles	P
Perfusion data ischemic			
Blood flow rest, mL/min/g	0.59 ± 0.21	0.84 ± 0.24	.09
Blood flow paced, mL/min/g	0.63 ± 0.11	1.00 ± 0.15	<.001
Perfusion data nonischemic			
Blood flow rest, mL/min/g	0.86 ± 0.32	0.94 ± 0.22	.66
Blood flow paced, mL/min/g	1.19 ± 0.45	1.33 ± 0.27	.66
Immunohistochemistry ischemic			
Isolectin B4 staining, % positive	21.1 ± 2.2	19.2 ± 1.9	.14
α-Smooth muscle actin, vessel count	11.7 ± 2.3	10.6 ± 3.5	.56
Immunoblotting ischemic			
AKT	1.00 ± 0.19	1.34 ± 0.21	.009
pAKT	1.00 ± 0.16	1.14 ± 0.13	.18
AKT ratio	1.00 ± 0.16	1.18 ± 0.11	.03
Angiostatin	1.03 [0.99-01.11]	0.94 [0.71-0.96]	.01
Cathepsin B	0.65 ± 0.21	1.76 ± 1.02	.03
Cathepsin D	1.00 ± 0.32	0.76 ± 0.13	.20
Cathepsin L	1.00 ± 0.31	0.86 ± 0.18	.52
Collagen 18	1.00 ± 0.27	0.60 ± 0.11	.01
Endostatin	1.00 ± 0.25	0.89 ± 0.34	.47
eNOS	1.00 ± 0.20	0.78 ± 0.15	.08
p-eNOS	0.86 ± 0.14	1.81 ± 0.32	<.001
eNOS ratio	0.74 ± 0.20	1.98 ± 0.76	.003
PI3K	1.00 ± 0.18	1.35 ± 0.11	.002
Plasminogen	1.00 ± 0.19	1.31 ± 0.31	.04
TIMP-2	1.00 ± 0.47	1.86 ± 0.70	.02
Immunoblotting nonischemic			
AKT	1.10 [0.78-1.12]	0.97 [0.91-1.10]	.71
pAKT	0.91 [0.82-1.24]	1.28 [0.92-1.33]	.10
AKT ratio	1.00 ± 0.27	1.13 ± 0.18	.31
Angiostatin	1.00 ± 0.10	1.05 ± 0.12	.43
Cathepsin B	1.00 ± 0.39	2.04 ± 1.35	.09
Collagen 18	1.00 ± 0.23	0.89 ± 0.25	.43
eNOS	1.00 ± 0.61	0.67 ± 0.48	.33
p-eNOS	1.00 ± 0.74	1.31 ± 0.58	.44
eNOS ratio	1.18 [0.04-1.93]	0.98 [0.93]	.32
PI3K	1.00 ± 0.23	1.60 ± 0.23	<.001
Plasminogen	1.00 ± 0.19	1.07 ± 0.10	.44
TIMP-2	0.76 ± 0.18	0.92 ± 0.42	.41

All of the data from the study. Data with a normal distribution are listed as mean ± SD. Nonparametric data are listed as median [Q1-Q3]. *AKT*, Protein kinase B; *p-AKT*, phosphorylated protein kinase B; *eNOS*, endothelial nitric oxide synthase; *p-eNOS*, phosphorylated endothelial nitric oxide synthase; *PI3K*, phosphatidylinositol 3-kinase; *TIMP-2*, tissue inhibitor of metalloproteinases 2.